

ABSORPTION LASER SPECTROSCOPY OF MOLECULES IN SHORT-WAVELENGTH REGION OF SPECTRUM

V.P. Lopasov

*Institute of Atmospheric Optics,
Siberian Branch of the Russian Academy of Sciences, Tomsk
Received January 22, 1997*

Physical ideas are set forth, high-priority results of investigation into overtone and combination molecular transitions are presented, and promising directions of investigations are pointed out.

INTRODUCTION

In the 300–1250 nm (8000–33000 cm⁻¹) short-wavelength region of spectrum the overtones and combination vibrational tones of most molecules of the outdoor atmosphere^{1–2} are located. The corresponding vibrational-rotational (VR) transitions are forbidden in the harmonic oscillator and rigid top approximations (further referred to as forbidden transitions), but are allowed due to anharmonicity effects, pairwise Coriolis interaction of vibrations in a rotating molecule, and VR interactions.^{1,3}

By the middle 60s, only measurements of positions of strong forbidden VR transitions of linear molecules, performed by Mecke⁴ and Herzberg⁵ with classical spectrometers with low resolution, were available. Theoretical analysis of the forbidden VR transitions of molecules reduced to fitting of calculated and experimentally measured frequencies by the combination difference method. Tunable lasers in the visible and near-IR ranges were lacking, but by that time the regime of frequency sweeping of a free-running neodymium-glass laser was realized and common features were noted that suggested broad potentialities for application of swept lasers to spectroscopy.⁶

The idea of investigation into the forbidden molecular transitions with the help of lasers appeared in 1966 as a consequence of directions of studying atmospheric optical properties by laser means developed by V.E. Zuev. It was well known that laser energy flux fields are much smaller by their magnitudes than intramolecular fields, but their effects are comparable, and in cases of resonance even larger than those of intermolecular interactions responsible for the relaxation processes and mixing of states. Therefore, of special interest were nonequilibrium conditions, when the effects of inter- and intramolecular interactions, relaxation processes, and exciting radiation fields on the probability of molecular transitions were comparable. A possibility opened to cooperate different techniques for forming of molecular transitions in such a way that the Markovian conditions of relaxation processes were violated and a molecule remembered its prehistory in case of new excitations. In this sense, the

overtones and combination VR transitions of molecules are favorable objects of investigation.

The problem of theoretical spectroscopy in the short-wavelength region was to develop the method for processing of the experimental data, which can consider resonance interactions of a large number (4–20) of high-lying VR states of molecule. In the experiment, the main problem was to obtain such regimes of laser generation that spectroscopic methods and means developed on their basis had the sensitivity, accuracy, and spectral resolution sufficient not only for registration of the forbidden VR transitions of molecule, but also for the investigation of their peculiarities.

1. PECULIARITIES OF THE FORBIDDEN VR MOLECULAR TRANSITIONS

1.1. Profound effects of the intramolecular and intermolecular interactions and the Doppler broadening of the parameters of absorption lines

For high-lying VR state of molecule, the high density of the power spectrum and the high amplitude of nuclear vibrations are typical and the spectral line profiles are strongly dependent on the molecular transition frequency. The first factor leads to multiple resonances and mixing due to intramolecular interactions of all the states with energies greater than a certain fixed value, the second – to the fact that the energy of VR interaction becomes comparable to the energy of rotational motion, and the third – to masking of the effects of the first two factors by the Doppler line profile.⁴

The forbidden VR spectrum is determined primarily by the effects of VR interaction and anharmonicity. In this case, local VR transitions between sufficiently higher states, which are intensified due to very small interference effects of anharmonicity and VR interaction, are important, but for exact coincidence of the energy levels.³ It is clear that resonances between high-lying states shift their energy levels and an increasing role of VR interaction in molecular dynamics diversifies the dependence of

broadening and shift of the individual line centers on the pressure, temperature, and external field.

Of special interest are spectroscopic investigations into nonequilibrium conditions, when the frequency of elastic molecular collisions exceeds Doppler's line width $\nu_{\text{col}} \geq D_d$ and these collisions change the velocity of radiative molecule, decreasing the linewidth with the increase of its intensity at the center due to the Dike effect.⁷ Because in the strong field the spectral and polarization inhomogeneities of a medium are manifested under nonequilibrium conditions, in addition to the Dike mechanism, other factors may take part in the formation of the line profile, in particular, relation between momenta of mass centers of interacting molecules, oscillator phase discontinuity on the transition, and effects considering the correlation between the width, shift, and intensity of the transition components, called phase effects.⁸ For frequency of elastic and inelastic collisions $\nu_{\text{col}} \geq D_d$ and Stark's splitting of transition levels by Δ , which does not exceed $1/T_{\text{col}}$, the collisions may be remained in phase memory in the form of superposition of certain stationary states formed in the interaction process. Field-induced phase memory contributed to the spectral exchange between the transition components,^{8,9} and the registered line profile depends on polarization of radiation¹⁰ interacting with the molecule on the length of free path and reading the information about the result of intermolecular interaction.

External field may intensify the Dike effect,¹¹ that is, play the same role as the increase of the elastic collision frequency. From the physical consideration, it is clear that the Dike effect in the short-wavelength region of spectrum should be less pronounced than the oscillator phase discontinuity on the transition and orientation of molecule in the process of collisions. Possible manifestation of other effects of intermolecular interaction through the forbidden VR-transition line profiles, especially in the external fields, depends on many factors and calls for special experimental and theoretical investigations.

1.2. Strong manifestation of Stark's and Zeeman's effects

The structure of VR transitions of molecules may be caused by intramolecular interactions and electric (E) and magnetic (H) fields of external sources. The forbidden molecular transitions possess weak forces of the oscillators. Here, the role of the effects connected with variations of the level population is insignificant; the level shift and splitting are of great importance. An external electrostatic field affects electron motion in the molecule (Stark's effect), breaking its symmetry about the inversion at the mass center, and depends quadratically on the field strength. The linear Stark effect is manifested only when the external field strength is sufficient for noticeable changes of molecular eigenstates existing without the field.¹² The magnitude of the Stark quadratic effect is inversely proportional to the level spacing and hence is increased with the decrease of the rotational state of molecule J .

The reason for the Zeeman splitting of the energy levels is that the magnetic molecular moments \mathbf{M} may be oriented in different ways with respect to the external magnetic field.¹ Additional energy of molecules with nonzero magnetic moments in the magnetic field H depends on the magnitude of its projection onto the \mathbf{M}_z component of the field. There are $g_j = 2J + 1$ different projections \mathbf{J}_z of the mechanical moment \mathbf{J} . Multiplicity of spatial degradation of the rotational level of molecule g_j determines the number of sublevels in the magnetic field and hence the maximum depth of the potential reservoir for the molecular momentum.

Contributions to the additional energy give the linear and quadratic Zeeman effects, that is, the interaction of orbital electron current of molecule with the external field (Zeeman's energy) and magnetic flux engendered by the induced current (diamagnetic or potential magnetic energy).¹² The diamagnetic energy is proportional to the mean area occupied by the electron density and hence the importance of the quadratic Zeeman effect is increased for high-lying electron, VR, and rotational states of molecule.

1.3. Strong manifestation of molecular polarizability in the external field

The molecule polarizability in the external electric field comprises static (electron and atomic) and orientational ones.¹² The orientational polarizability is connected with the change of molecular rotation and its contribution D_{rot} to the total polarizability of a polar molecule exceeds $\Delta E_{ij}/B_e \approx 1000$ times the contribution from the perturbation of electron motion. Here, ΔE_{ij} and B_e are the difference of electron level energies and the rotational constant of the molecule, respectively. However, after an averaging over the orientations it becomes clear that the resulting value $\langle D_{\text{rot}} \rangle$ remains nonzero only for the molecules with zero moments.¹² Hence, the effect of orientation of molecules in the lowest state $|J = 0, M = 0\rangle$ in external electric field reaches its maximum.

In the linearly polarized optical field, whose intensity satisfies the condition $I \geq cB_e/\pi(\alpha_{\parallel} - \alpha_{\perp})$, where α_{\parallel} and α_{\perp} are the longitudinal and transverse polarizabilities of the molecule, the rotating molecule is oriented in the plane perpendicular to the direction of the field E . In this case, rotational levels¹³ are rearranged, spacings between them are increased, and the rotational relaxation cross sections are decreased. Spatial orientation of molecules induced by the resonant light is related in Ref. 14 with the sharp increase of the static gas polarizability and depends on the exciting radiation frequency detuning from the optical transition. In Ref. 15, the mechanism of induced orientation of molecules in the resonance field is associated with collisions and is explained by different relaxation rates of polarization moments of working transition levels.

In Ref. 16, it was established that nonlinear polarization of molecules caused by the Stark quadratic effect and the effect of change of the level population difference on the nonresonant polarization may reach large magnitudes. This nonlinear polarization is especially great for weak lines when the difference of tensors of the Stark level shifts $|\delta_i - \delta_j|$ is comparable to the polarizability of the resonant transition $|D_{ij}|^2/\gamma_{ij}h$ or when the difference between the Stark shifts of working levels is comparable to the frequency difference of the exciting radiation (biharmonic); here, D_{ij} and γ_{ij} are the dipole moment of the molecular transition and width of the molecular line, respectively.

Optical biharmonic propagating through the medium induces not only polarization waves of the order $n=0$ at frequencies ω_1 and ω_2 but also the polarization waves of the order n at frequencies $\omega_j = \omega_1 \pm n\delta$ and $\omega_i = \omega_2 \pm n\delta$, where $\delta = (\omega_1 - \omega_2)/2$ (see Ref. 16), in the molecular medium. The polarization waves of the order $n=1$ in the molecular medium engender a number of coherent and nonlinear effects.

Based on some of these effects caused by molecular and induced polarization resonances at the difference biharmonic frequency $\delta = (\omega_1 - \omega_2)/2$, new directions of molecular spectroscopy were developed, in particular, coherent active Raman spectroscopy (CARS) methods¹⁷ and amplitude-phase modulation spectroscopy methods.¹⁸ By contrast, effects of the Stark bistability and of the Stark phase advance of the AS-signal that are manifested when the frequency difference goes through the VR-transition,¹⁶ of parametric wave interaction,²⁰ and of vortex combination phenomena²¹ are developed only weakly.

To produce effects of the last type, several resonances of the biharmonic polarization waves of the order $n=1$ with molecules of the medium are necessary. These effects are characterized not only by the probability of filling of any level (basic mechanism for the working levels of the long-wavelength region), but also by multipole moments of higher rank.²² They are sensitive to field-induced shifts of the working levels, their splitting into magnetic sublevels, and relaxation in the system of magnetic sublevels, as well as to natural and induced molecular anisotropy and to the vector character of radiation and its polarization state. Hence, it is precisely these effects that may be manifested on the forbidden VR transitions, keep the phase memory in the form of superposition of nondegenerate magnetic sublevels, and transform the registered profiles of molecular lines.

Moreover, because the effects of centrifugal distortion of the molecular level structure depends on the even number (four, six, eight, and so on) of rotational disturbances,¹³ the possibility of activation of individual forbidden VR transitions through resonance parametric molecular interactions of the order $2n$ with the field of the optical biharmonic must not be ruled out. In this case, the probability of internal

transitions of the quantum system may be increased by external field.²³

2. RESULTS OF INVESTIGATIONS

2.1. Spectrum of the atmosphere

The intensity of the forbidden VR absorption bands of a molecule is by 5–6 orders of magnitude weaker than the fundamental VR bands located in the IR region. With classical absorption spectrometers, such weak bands could be recorded with high spectral resolution (≤ 1 nm) only for long atmospheric paths. Therefore, pioneer experimental results of investigations are compiled in atlases of solar spectrum^{24–26} and absorption spectrum of the atmosphere measured with an intracavity laser spectrometer²⁷ (ICLS). Most lines in these atlases were attributed to the water molecule absorption spectrum.

The bank of spectroscopic atmospheric data created in the 70s encompassed only the fundamental VR transitions of molecules in the near-IR region. By now, the automated data bank capable of storage, search, sampling, and calculation of various spectroscopic molecular characteristics has been created.²⁸ It also encompasses the short-wavelength region.

2.2. Spectroscopy of intramolecular interactions

First mass measurements of the water molecule absorption spectrum in the short-wavelength region of spectrum were carried out with an optoacoustic laser spectrometer (OALS) with resolution of $5 \cdot 10^{-4} \text{ cm}^{-1}$ and sensitivity of 10^{-9} W/cm . The totality of 282 H_2O absorption lines was detected in the 16500–16900 cm^{-1} spectral range¹ (Fig. 1).

To identify and to analyze theoretically the recorded spectrum, the effective rotation matrix with superposition of higher vibrational states (401), (321), (500), and (420) was constructed. The vibrational, centrifugal, and resonance constants were then determined by minimization of the functional comprising experimental and theoretical energies of the VR levels of higher vibrational states and the number of the sought-after parameters and working levels of the molecule. In this case, 223 from 282 lines were identified; in so doing, the VR energy levels for the first three of the above-indicated vibrational states were determined up to $J = 7-9$.

The broadband ICLS and the narrow-band OALS were capable of recording further several tens of new bands and several thousands of absorption lines of H_2O , HDO , and D_2O in the 8000–12000 and 16500–16900 cm^{-1} regions.^{31–33} A theoretical analysis of asymmetric molecular spectra was made to interpret the recorded spectra and to determine the energy levels and the rotational, centrifugal, and resonance constants of higher vibrational states, including (230), (032), and (041) of H_2O , (030), (130), and (031) of D_2O , and (050), (051), and (005) of HDO .

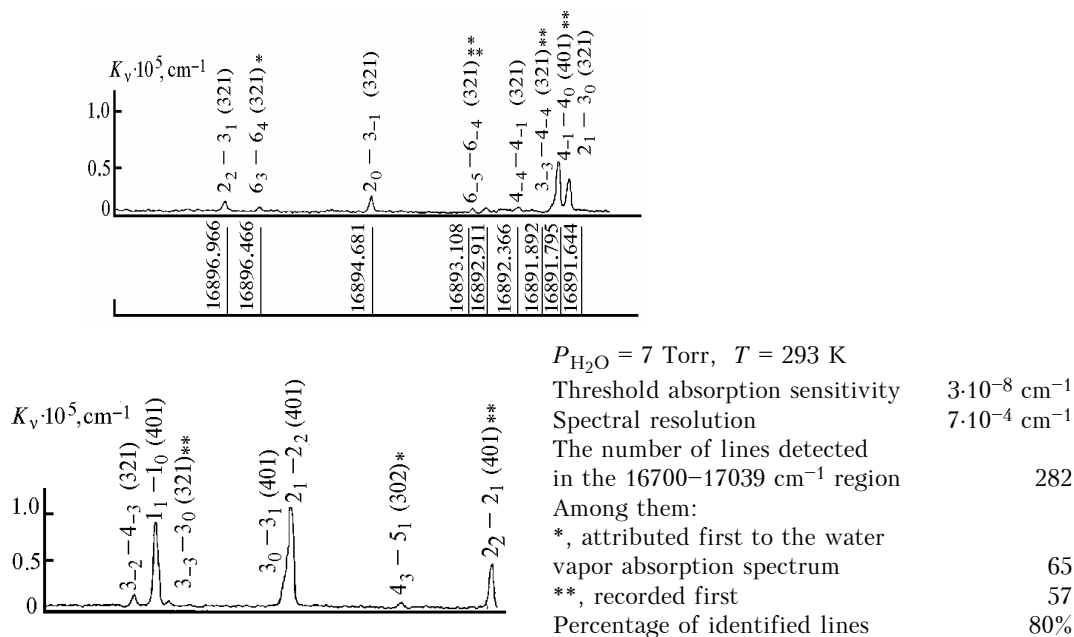


FIG. 1. Water molecule absorption spectrum.

Systematic mixing of states formally belonging to different polyads due to intramolecular interactions was revealed and disturbances of their energy distribution were explained. Results of theoretical solutions to the inverse spectroscopic problems were generalized in Ref. 34 along with techniques for interpreting the forbidden VR spectra of the water molecule and its isotopes.

Absolute values of intensities of some water molecule absorption lines were determined by calibration of the OALS and ICLS by way of comparison of the parameters of individual lines measured with these spectrometers and with laser spectrometer under identical conditions.

Combined experimental and theoretical investigations into the forbidden VR transitions of the H_2O molecule revealed the manifestation of bending-rotational interaction in this molecule.³⁵ This effect consists in mutual disturbances of higher VR states belonging to different resonance polyads. It combines the vibrational states with energies in excess of 8000 cm^{-1} in one polyad of interacting states. A local resonance (called the HEL resonance) occurs between higher VR states, which transforms two quanta of valence vibrations into five quanta of bending vibrations. Excitation of soft bending vibration in the water molecule causes the change of the centrifugal constants several hundred times; therefore, their traditional representation in the form of linear and quadratic functions of the vibrational quantum numbers becomes inadequate. Consideration of the HEL resonance in theoretical analysis of the H_2O absorption spectrum increases the precision of identification of the

VR transitions and determination of the molecular constants.

At present the above results are essentially supplemented by measurements of the absorption spectra of H_2O isotopes and H_2S molecules at frequencies up to 25000 cm^{-1} performed with the Fourier spectrometers in USA and France³⁶ and with the ICLS in Russia (IAO SB RAS). At the IAO SB RAS, the spectrum was identified by the method of isotopic substitution³⁷ and thorough description of higher VR state of these molecules was given on the basis of the experimental data on the transitions between low-lying VR states. Herzberg⁵ started experimental investigations into the absorption spectra of linear molecules in the 30s using a classical spectrometer with lower resolution and sensitivity. These investigations were continued at the IAO SB RAS in the middle 70s. New combination absorption bands of linear molecules CO_2 , C_2H_2 , and N_2O were revealed in the $9190\text{--}9500 \text{ cm}^{-1}$ range^{38–39} using the broadband and narrow-band ICLSs. In particular, absorption lines of combination bands 12^03 and 04^03 possessing large rotational quantum numbers J were recorded. The positions of lines of the hot band $13^13\text{--}01^10$ with J up to 44 were first recorded under laboratory conditions. In the C_2H_2 spectrum, the perpendicular band 12003^1 at 407.74 cm^{-1} and the lines of the three branches of the band 21001^1 at 9366.61 cm^{-1} were first revealed. The intensity of strongest absorption lines S_j was $10^{-6} \text{ cm}^2 \cdot \text{atm}$. An example of fitting the data obtained with a highly sensitive broadband ICLS and with a narrow-band ICLS having high resolution, both using a Nd-glass lasers,³⁹ is shown in Fig. 2.

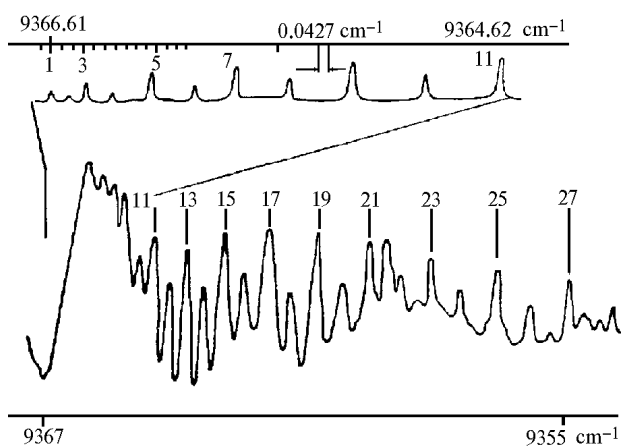


FIG. 2. Absorption spectrum of C_2H_2 molecule recorded with the broadband and narrow-band laser spectrometers.³⁹

The width of the emission spectrum of the narrow-band laser was less than 2 MHz. A Fabry-Perot

interferometer 129 cm long²⁹ was used to measure the emission spectrum width. Rotational structure of the absorption bands of linear molecules is weakly mixed due to intramolecular interactions. For this reason, the recorded absorption spectra of CO_2 , C_2H_2 , and N_2O molecules were analyzed with the help of the combination difference method capable of separating between lower and higher states of transitions, determining the rotational, centrifugal, and resonance constants, and estimating the energies of higher vibrational states.

In the last 10 years, the absorption spectra of the water molecule isotopes and molecules of carbon dioxide, C_2D_2 , C_2HD , N_2O , CH_4 , C_2H_2 , NH_3 , HBr , and H_2 were recorded in the 8000–18000 cm^{-1} range. Many unknown bands were revealed, among them hot absorption bands; some absorption bands are shown in Fig. 3.

The idea of thorough description of higher VR states (up to 15000 cm^{-1}) and spectra of triatomic linear molecules CO_2 and N_2O was realized in Ref. 43 based on the experimental data about the transitions between the lower VR states (see Table I).

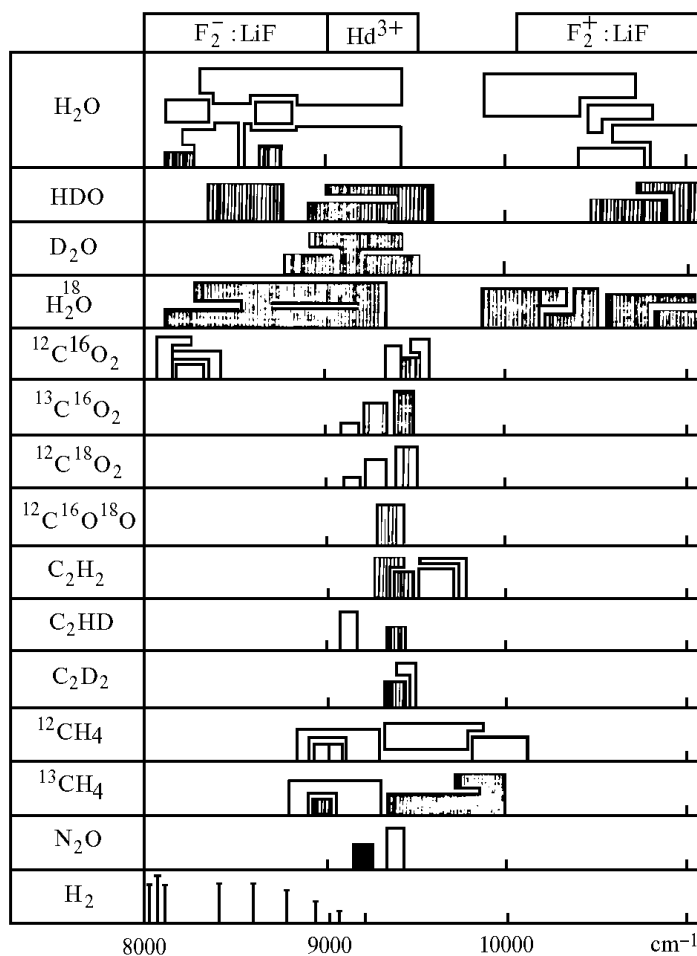


FIG. 3. Molecular absorption bands recorded with the ICLS in the 8000–11000 cm^{-1} range⁴⁰ (hatched regions indicate the bands recorded first).

TABLE I. Predicted and experimental (Camparque et al.⁴³) values of the spectroscopic constants G_V and B_V of the N_2O molecule.

State	$G_V^{(exp)}$	$G_V^{(exp)} - G_V^{(calc)}$	$B_V^{(exp)}$	$B_V^{(exp)} - B_V^{(calc)}$
00 ⁰ 4	8714.117	- 0.061	0.40518	0.00000
12 ⁰ 3	8877.028	0.337	0.40800	- 0.00001
20 ⁰ 3	8976.197	- 0.004	0.40512	- 0.00023
10 ⁰ 2 a	9219.035	0.323	0.40717	- 0.00042
10 ⁰ 2 b	9294.966	- 0.206	0.40618	- 0.00066
60 ⁰ 1	9606.305	- 0.623	0.40724	- 0.00081
10 ⁰ 4	9888.579	0.210	0.40333	- 0.00008
30 ⁰ 3 a	10079.560	0.621	0.40616	- 0.00013
30 ⁰ 3 b	10163.614	- 0.016	0.40369	- 0.00040
50 ⁰ 2	10429.117	0.366	0.40515	- 0.00056
00 ⁰ 5	10815.274	0.769	0.40424	- 0.00052
01 ⁰ 4	10820.113	- 0.282	0.40473	0.00061
02 ⁰ 5	11844.970	1.130	0.40378	- 0.00004
10 ⁰ 5	11964.252	0.573	0.40009	0.00018
00 ⁰ 6	12891.153	0.038	0.39838	- 0.00044
10 ⁰ 6	14009.686	1.709	0.39657	0.00005
00 ⁰ 7	14931.267	1.116	0.39178	0.00013

Note: All quantities are in cm^{-1} .

2.3. Spectroscopy of intermolecular interactions

Broadening the water molecule line [in the band 000–103 on the transition $4_{-3} \rightarrow 5_{-4}$ at 694.38 nm] by the N_2 pressure was studied using a high-speed high-resolution (30 MHz) spectrophotometer with the linearly polarized radiation of a ruby laser.⁴⁴ The spectrophotometer also comprised a 30-m multipass cell, which provided path lengths up to 4 km, a DSF-8 spectrograph, a stabilized He-Ne laser, and an array of

the Fabry–Perot interferometers with photographic and photoelectron recording of the temporal radiation spectrum.⁴⁵ Careful calibration of an electronic channel of the radiation intensity measurement ensured 1 and 2% errors of measuring the transmission for continuous and pulsed radiation, respectively.

It was found that at $P_{H_2O} = 3$ Torr and $P_{tot} = 20$ Torr, the Doppler line profile was transformed into the dispersion one, but without its narrowing due to the Dike effect (Fig. 4).

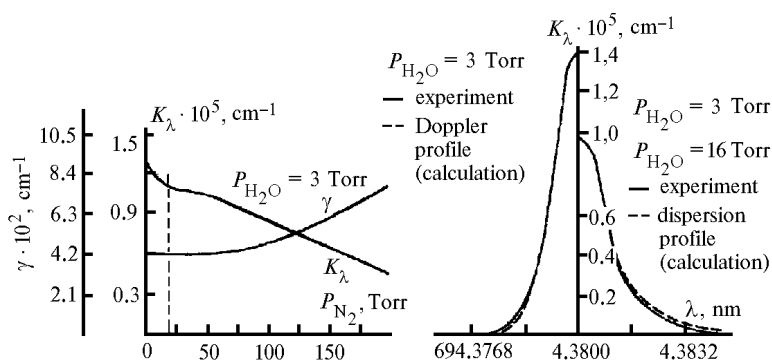


FIG. 4. Measurements of the parameters of the water molecule line at 694.38 nm in nitrogen under nonequilibrium conditions.

The linewidth remained unchanged within the limits of the experimental errors (1–2%) until the total pressure increased up to $P_{tot} = 50$ Torr with the noticeable decrease (in contrast with the Dike effect) of the absorption coefficient at the line center. The difference between the measured and calculated parameters may be due to neglect of contribution from collisions to the change of projections

M_i and M_j of angular momenta J_i and J_j of the working transition levels for the theoretical model.

A comparative analysis of measurements of broadening of the water vapor absorption line at 694.38 nm by the pressure of foreign gases performed with laser spectrometer, OALS, and broad-band ICLS (Fig. 5) was made in Ref. 46.

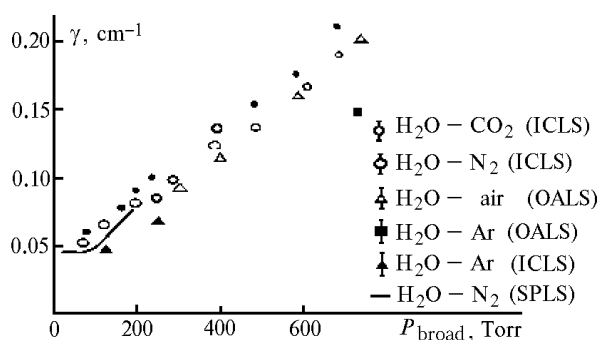


FIG. 5. Broadening of the water molecule line at 694.38 nm by foreign gas pressure measured with different spectrometers.

When the pressure P of N_2 , air, or CO_2 is less than $P = 760$ Torr, the results of measurements of the coefficients of broadening $\gamma(p)$ agree well. The coefficients of collision broadening of the water molecule absorption line by the pressure of these gases are well correlated with their quadrupole moments, but are somewhat underestimated at pressures $P \geq 200$ Torr in comparison with lower pressures. This experimental fact can be attributed to statistical redistribution of the parameters characterizing the phase and Dike effects.

The line center shift due to intra- and intermolecular interactions is of not only fundamental, but also applied importance.⁴⁷ The H_2O absorption line center shift at 694.38 nm by the air pressure was recorded with a two-channel OALS on a ruby laser.⁴⁸ As the air pressure increased from 50 to 750 Torr, the 694.38 nm line center shifted toward longer wavelengths with a rate of 0.76 ± 0.04 MHz/Torr. Analogous result was obtained for the water molecule absorption line at 1074.76 nm using a narrow-band ICLS (see Ref. 48). As the air pressure increased to 400 Torr, the 1074.76 nm line center shifted toward longer wavelengths with a rate of 0.91 ± 0.06 MHz/Torr. The experimental and theoretical line shifts were fitted only after consideration of the molecular polarizability not only in the lower, but also in the upper VR states.

Now these investigations are essentially supplemented by measurements of the absorption spectra of H_2O and H_2S molecules at frequencies up to 1700 cm^{-1} with the use of the Fourier spectrometers. It was revealed that the position of levels depends on the rotational quantum number J ; theoretical analysis of the pressure-induced line shifts was made for different physical models (private communication from Dr. L.N. Sinitsa, IAO SB RAS).

2.4. Spectroscopy of nonlinear interactions

The OALS can be used to study both linear and nonlinear optical characteristic of gases, because a highly intense optical field can be easily made

homogeneous along a cell of an opto-acoustic detector. In case of resonance interaction of radiation with gas, its absorptivity depends in a complex way from the radiation intensity and frequency and ratios of the radiation pulse duration to the relaxation times T_1 , T_2 , t_v and t_r (here, T_1 and T_2 are the longitudinal and transverse relaxation times of the transition and t_v and t_r are the vibrational and rotational relaxation times).⁵⁰ This dependence can be correctly taken into account based on the results of numerical analysis of the signal amplitude of the opto-acoustic detector made in Ref. 51.

Nonlinear dependence of the spectral distribution of the absorption coefficient across the line profile at 694.38 nm, corresponding to the degenerate transition $4_{-3} \rightarrow 5_{-4}$ of the H_2O molecule band $000 \rightarrow 103$, on the intensity of the quasimonochromatic (0.03 cm^{-1}) laser radiation at different air pressures was observed in Refs. 52–54 using the OALS on a ruby laser (Fig. 6). The quantity $A(I, \lambda) \sim E_{abs}/E_0$ specifies the signal recorded under conditions of quasistationary nonlinear absorption ($T_p = 30$ – 40 ns).

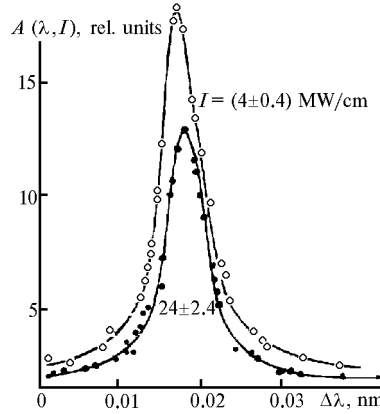
The effect of absorption saturation at the line center was the greater, the lower was the pressure of the examined medium. However, in this case the line broadening, typical of the saturation effect in monochromatic radiation field, was not observed. The tendency for a line narrowing in a strong field was also revealed in the experiment; the difference between the calculated and measured linewidths reached $0.3\gamma_0$ ($\gamma_0 = 0.15$ cm^{-1}), which goes far beyond the limits of measurement errors. The saturation parameter E_s , estimated from the dependence of $A(I, \lambda)$ in the absorption line center by the technique reported in Ref. 55 at the air pressure $P = 270$ Torr, was (3.2 ± 0.5) J/cm². This value is by an order of magnitude greater than the saturation parameter calculated from the dipole moment.

Table II lists the physical mechanisms that explain the narrowing of the water molecule collision line at 634.38 nm in a strong field. Estimates of the orders of magnitudes show that at $I = 35$ MW/cm² and $P_{tot} = 300$ Torr the times required for mutual orientation of the H_2O , N_2 , and O_2 molecules and changing of the contribution from elastic collisions to the line broadening is quite comparable to the mean free time of the molecules $\tau_{free} = 10^{-10}$ s. The conditions of the experiment also suggest the contribution from multiphoton processes on degenerate transition to the linewidth.

Moreover, high sensitivity of the forbidden VR molecular transitions to the molecular polarizability in the external field is also manifested across the linewidth. This is indicated by the measurements of nonlinear absorption at the same line performed in Refs. 53 and 54 for binary mixtures H_2O – air, H_2O – N_2 , and H_2O – Ar using differently polarized high-power exciting radiation with a two-channel OALS (Fig. 7).

Dependence of the parameters describing the line profile $A(\lambda, I)$ on the radiation intensity for the H_2O absorption line at 694.38 nm

Buffer gas	P , Torr	I_{las} , MW/cm	$A^{\text{max}}(I)$, rel. units*	γ_{meas} , $\text{cm}^{-1} \text{cm}^{-1} \text{cm}^{-1}$ (**)
Air	750	5 ± 0.5	6.5	0.20
	500	35 ± 3.5	5.1	0.21
		3 ± 0.3	9.5	0.16
		8.5 ± 0.8	8.5	0.17
	270	25 ± 2.5	7.6	0.17
		5 ± 0.5	10.7	0.11
		35 ± 3.5	6.0	0.10
Nitrogen	470	6 ± 0.6	6.5	0.14
	300	23 ± 2.3	5.5	0.13
		4 ± 0.4	8.0	0.11
		24 ± 2.4	5.6	0.10
Argon	470	4 ± 0.4	6.8	0.09
	300	20 ± 0.2	5.8	0.11
		4 ± 0.4	12.2	0.06
		21 ± 2.1	7.0	0.08



*Error in measuring A^{max} , in relative units, does not exceed 5%.

**By γ_{meas} , the total width of the distribution $A(\Delta\lambda)$ at $0.5 A^{\text{max}}$ is meant.

FIG. 6. Nonlinear absorption in the water molecule line at 694.38 nm in nitrogen³³ at $P_{\text{tot}} = 300$ Torr.

TABLE II. Physical factors leading to the narrowing of the collision profile of absorption line.

Mechanism	Conditions of realization, characteristic parameters	Value of the parameter at $I = 35 \text{ MW/cm}^2, P_{\text{tot}} = 300 \text{ Torr}$
1. Change of the molecular interaction cross section due to orientation of molecules in a strong field.	$\frac{\tau_{\text{or}}}{\tau_{\text{free}}} \approx N \bar{\sigma} \bar{v} \sqrt{\frac{(\alpha_{\parallel} - \alpha_{\perp}) E_l^2}{M a_0^2}} < 1$	0.1 – 1
2. Intensification of the Dike effect. ¹¹	$\gamma_{12} / k \bar{v} \leq 1$	1
3. Nonmonochromaticity of radiation and multiphoton processes.	$V_{ij} / \delta\omega_1 \geq 1$	2
	$\delta\omega_1 / \gamma_{12} \geq 1$	1
4. Change of the transition cross section due to redistribution of the rotator levels in a strong field.	$\frac{(\alpha_{\parallel} - \alpha_{\perp}) E_l^2}{chB_E}$	$10^{-3} - 10^{-4}$
5. Elimination of phase discontinuity in a strong field. ⁹	$\gamma_{12} / v_{\text{col}} \sim 1$	0.5
	$V_{ij} T_{\text{col}} \geq 1$	10^{-2}

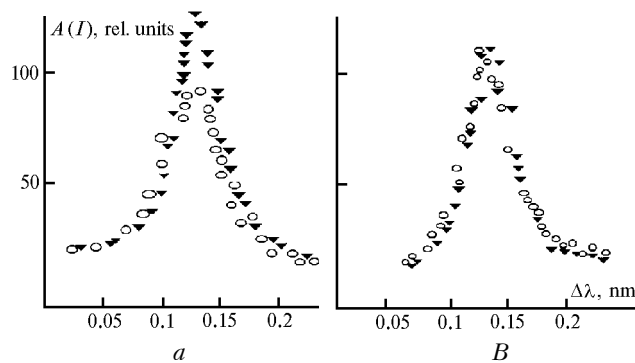


FIG. 7. Spectral dependence⁵⁴ of the energy of linearly (a) and circularly (b) polarized ruby-laser radiation absorption in the line at 694.38 nm: \blacklozenge , $I = 5 \text{ MW/cm}$; \circ , $I = 35 \text{ MW/cm}$.

The absorption at the line center remained unchanged as the intensity of the exciting circularly polarized radiation increased from 5 to 35 MW/cm², whereas the results of the previous experiment were confirmed for the linearly polarized exciting radiation. In the mixture of H₂O with Ar, whose atoms have no permanent electric moments, the saturation of absorption at the line center was revealed along with the line broadening, as it was the case when we considered the saturation on the VR transition.

2.5. Qualitatively new results

The first high-speed laser spectrometer on a ruby laser with thermal and electrooptical tuning of the wavelength generated by the laser and a multipass gas cell with the optical White system capable of obtaining path lengths up to 300 m when mirrors were spaced at 5.5 m was put into operation in 1970. The tuning frequency step was limited from below by the intermode spacing and from above – by the width of uniform gain of an active medium. In the nonstationary regime of operation, the laser generated biharmonic, that is, two sets of frequencies ~ 300 MHz wide spaced at ~ 300 MHz with the intensities that differ ten times.

With this laser spectrophotometer, 8 new unstable absorption lines were revealed and the H₂O absorption line at 694.38 nm. The repetition frequency of double spikes of a laser pulse was 5 MHz and the spectrum width of the linearly polarized radiation was 300 MHz (Fig. 8, block diagram of the spectrophotometer is shown at the upper right of the figure).

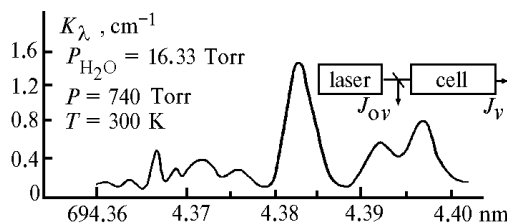


FIG. 8. Spectrum of unknown lines of the atmospheric water vapor measured with a high-speed spectrometer with biharmonic ruby-laser radiation.

The absorption coefficient of molecular medium ($P_{\text{H}_2\text{O}} = 16.35$ Torr, $P_{\text{air}} = 740$ Torr, and $T = 300$ K) was estimated from the attenuation of a stronger component of the biharmonic with the error 8–10 % (see Ref. 56). The width of the unstable lines was two times less than the width of the collisional line and the profile of the line at 694.38 nm was deformed: the line center was shifted toward longer wavelengths, the linewidth was halved, and the absorption at the line center doubled in comparison with the data of Ref. 57. Later these absorption lines of the H₂O molecule were not recorded with a quasimonochromatic OALS, broadband ICLS, and narrow-band spectrophotometer.

I put forward a hypothesis³¹ that the unstable absorption lines in the region of generation of a ruby laser

under conditions close to the atmospheric ones are caused by a nonlinear parametric (multifrequency) resonance between extremely weak forbidden VR transitions of the H₂O molecule (their existence was pointed out by Dr. O.K. Voitsekhovskaya from the Tomsk State University in private communication) and optical biharmonic spaced at about 300 MHz, whose carrier frequency is tuned with a rate of 10³ MHz/μs. A salient feature of this resonance is that the transition probability depends not only on the amplitude, polarization, and frequency of the radiation components, but also on their initial phase difference.⁵⁸ The multifrequency resonance intensifies the extremely weak absorption lines of the H₂O molecule under atmospheric conditions, redistributing the energy of its interaction with the biharmonic over the spectrum and direction and increasing the probability of the VR transition $4_{-3} \rightarrow 5_{-4}$ of the band 000–103 of the H₂O molecule through the amplification of the Dike effect. That is, the biharmonic field intensifies the contribution from weak intramolecular interactions and elastic collisions to the molecular transition probability.

This hypothesis was formulated as a consequence of measuring the absorption by H₂O molecules in the line at 694.38 nm using the broadband ICLSs with long cavities ($L = 10$ m, intermode spacing was 15 MHz) and dynamic Stark cells inserted in semiconfocal half-meter cavities of ruby lasers (spacing of transverse modes was several units of MHz). The electric field amplitude on the capacitor plates of the second ICLS was varied from 50 to 300 V/cm and its frequency was changed from 1 to 20 MHz, which was typical of the repetition frequency of spikes generated by the free-running laser⁵⁶ and intermode spacing of the semiconfocal laser cavity.⁵⁹

In the first case, a signal with narrow spectrum detuned toward longer wavelengths from the absorption line center was generated in the dip of the ruby laser radiation caused by the H₂O absorption line at 694.38 nm (Fig. 9, block diagram of the ICLS is shown to the right; these results are unpublished). In the second case, it was revealed⁵⁹ that the depth $I(0)$ and the width γ_{dip} of the dip are the functions of the frequency Ω (Fig. 10, block diagram of the ICLS is shown to the right).

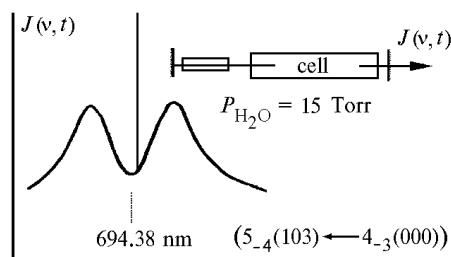


FIG. 9. Signal with a narrow spectrum generated in the dip of broadband ruby-laser radiation formed due to the water molecule absorption line at 694.38 nm.

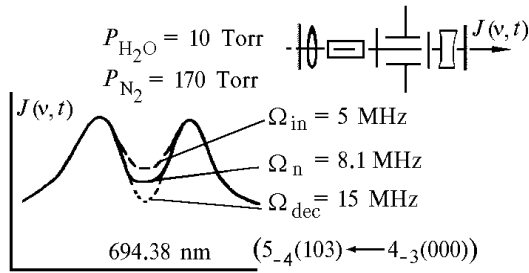


FIG. 10. Transformation of the dip profile of the broadband ruby-laser radiation caused by the 694.38-nm absorption line of the water molecules placed in the dynamic Stark cell.

In the field 300 V/cm, the maximum increase of γ_{dip} and decrease of $I(0)$ were observed at the frequency $\Omega_{\text{in}} = 5$ MHz, whereas the maximum decrease of γ_{dip} and increase of $I(0)$ – at the frequency $\Omega_{\text{dec}} = 15$ MHz; the deformation of the dip profile changed its sign at the frequency $\Omega_{\text{n}} = 8.1$ MHz. The parameters $I(0)$ and γ_{dip} changed by 10–15% when the measurable quantities changed by 4%. The neutral frequency Ω_{n} depended quadratically on the field amplitude.

A qualitatively new result is the HEL resonance³⁵ revealed in the H_2O molecule. It is due to much greater values of constant A_e for the vibrational states (070) and (170) than for the states (220) and (122). In this case, the rotational levels of the states (070) and (170) approach the rotational states (220) and (122) and at $K_a = 1$ the levels of two states get close, thereby engendering the resonance. This bending-vibrational interaction affects strongly the spectrum of weak forbidden VR bands of the H_2O molecule, intensifying the lines and changing the coefficient and even the sign of the line shift in comparison with the lines of the fundamental bands.

If the vibrational state 103 of the H_2O molecule ($\nu > 14400 \text{ cm}^{-1}$) is tuned to one of these local intramolecular resonances, this will verify the hypothesis that the extremely weak forbidden VR transitions intensify due to the parametric (multifrequency) resonance of the order $n = 1$ induced in the molecule by the optical biharmonic field.

The fluorescence band with the quantum yield $\eta_{270} \approx 0.01$ and the corresponding absorption band of the H_2O molecule with the absorption coefficient $K_{270} \approx 3 \cdot 10^{-5} \text{ cm}^{-1}$ were experimentally revealed in Ref. 60 under conditions of the free atmosphere and in Ref. 61 in the pure water vapors at $P_{\text{H}_2\text{O}} = 0.01\text{--}18$ Torr. The absorption bands at $\lambda_a = 230\text{--}320$ nm and the fluorescence bands at $\lambda_f = 280\text{--}400$ nm (Fig. 11) are located in the region of the forbidden VR transitions of the ground electron state of the H_2O molecule and are continuous in character.

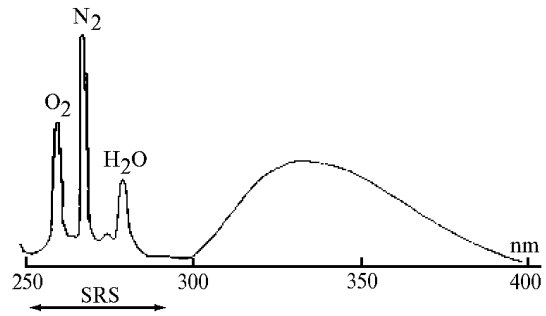


FIG. 11. Emission spectrum of the atmosphere.⁶⁰

Direct proportionality of the fluorescence intensity of the water vapor molecules to the temperature and pressure established in Ref. 62 indicates monomolecular rather than dimer nature of the revealed bands (Fig. 12).

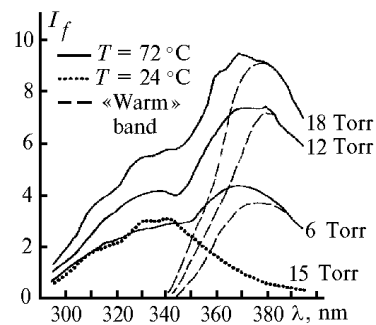


FIG. 12. Fluorescence spectrum of the water vapor molecules.⁶²

Klimkin and Fedorishchev⁶⁰ believe that the revealed band corresponds to the H_2O molecule transition to the repulsive state with $E_r = 37000 \text{ cm}^{-1}$ and high anharmonicity of the radiating transition.

Al'tshul' et al.⁶³ theoretically showed that the resonance propagation of three waves satisfying the conditions of the Rabi resonance through a two-level medium is accompanied with the formation of wave feedback and bifurcation character of their interactions. This effect of parametric interaction of two weak waves and the intense wave cannot be described in the strong fixed-field approximation. The revealed effect can be used to quench (intensify) the molecular absorption of the amplitude-modulated laser radiation for the given parameters of the external field and the medium.

Interesting possibilities are opened by the effect of nonlinear interference of polarizations induced by the resonant monochromatic radiation in a multilevel system comprising N sublevels of the ground and nondegenerate excited levels reported in Ref. 64. As spacings between the sublevels of the system are decreased, a giant line shift and suppression of continuum absorption occur, which are increased with the increase of the exciting radiation

intensity and the decrease of the pressure of the molecular medium. This effect can be used to extract information about the structure and magnitude of splitting of the ground state, the relaxation constants of low-frequency forbidden transitions, and the volume of the phase memory of the laser radiation having the narrow spectrum.

2.6. Conclusions

Summarizing the results of investigations into the forbidden VR transitions of molecules, it should be pointed out that the available experimental and theoretical data have already confirmed in many respects the above-discussed peculiarities in the formation of the parameters of the corresponding absorption lines.

In particular, the effects of the weak intramolecular resonance and polarization of the H₂O molecule induced by the external field on the center line intensity (amplification) and shift of the forbidden VR transitions by the gas pressure are experimentally recorded and theoretically substantiated. The experimentally revealed absorption and fluorescence bands of the H₂O molecule demonstrate a profound effect of intramolecular interactions, such as anharmonicity interference and VR interactions, on the forbidden VR transitions. Significant contributions from the field, polarization, and phase effects to the intensity and profiles of the absorption lines are evident from the experimental data on the broadening of the H₂O molecule line at 694.38 nm in weak and strong laser fields under conditions close to nonequilibrium as well as from the theoretical data on parametric coupling of three waves propagating through a two-level medium and polarization interference in a multilevel system at lower gas pressures.

Measurements of the H₂O molecule absorption spectra in the region of generation of a ruby laser performed occasionally or specially under nonequilibrium conditions demonstrate the cooperative effect of intra- and intermolecular interactions, field, and polarization.

3. DIRECTIONS OF FURTHER INVESTIGATIONS INTO ABSORPTION MOLECULAR SPECTROSCOPY IN THE SHORT-WAVELENGTH REGION OF SPECTRUM

Undoubtedly, we will be witnesses of an integrated experiment on studying the manifestation of the intramolecular interactions on the forbidden VR transitions, when the Fourier spectrometers and controllable laser sources will become standard tools in the short-wavelength region of spectrum.

A theoretical analysis of these experimental data for adequate physical models will make it possible to reveal the entire spectrum of the local intramolecular resonances between high-lying VR states considering the intermolecular interactions and the polarization of molecule induced by the external field.

It will become possible to predict the reference points on the frequency scale, in the vicinity of which the superposition of intramolecular effects may form new stable molecular states. The results of these

fundamental investigations will fill the data bank with the spectroscopic information.

Another promising direction of molecular spectroscopy may be intensification of the forbidden VR transitions due to the cooperative effect of intra- and intermolecular interactions and parametric perturbation of VR motions of the molecule upon exposure to polychromatic radiation under nonequilibrium conditions. It will be possible to control the intramolecular dynamics and to decrease or increase the intensities of lines corresponding to the given forbidden VR transition upon exposure to the external field. Of special interest are the effects of molecular deformation due to its proper rotation and resonance excitation of the even number of rotational motions in the external field. Because the rotational molecular Hamiltonian of a given vibrational state in this case also comprises the terms that depend on the fourth, sixth, and so on powers of the angular momentum, the effects of centrifugal distortion must be intensified in the external field and must deform the molecule in the process of its coherent interaction with the external field.

And finally, spectroscopy of nonstationary states may be promising. By this term we mean the process of adaptation of the molecule-rotator and the field of the exciting biharmonic accompanied by accumulation of the phase advance of the rotational RS, for example, due to the Stark vibration of the lowest $|J=0, M=0\rangle$ rotational level and the Zeeman decay of the higher $|J, M\rangle$ rotational level of the molecule. In this case, the phase transition of the molecule-rotator to a supermultiplet "molecule + field" should occur at the preparatory stage comparable to the period of rotation of nuclei with respect to each other. The molecule should translate from the ground EVR state to the spin state formed by the magnetic sublevels of the rotational level $|J, M\rangle$ (see Ref. 65). Successive development of this direction will make it possible to obtain the electromagnetic fields with large momentum⁶⁶ and to analyze with high accuracy the isotopic composition of the molecular medium.

ACKNOWLEDGMENTS

I would like to acknowledge Dr. M.M. Makagon for his valuable remarks and help in preparation of this paper.

The work was supported in part by the Russian Foundation of Basic Researches, Grant No. 96-05-64283.

REFERENCES

1. G. Herzberg, *Vibrational and Rotational Spectra of Polyatomic Molecules* [Russian translation] (Foreign Literature Press, Moscow, 1949), 647 pp; M.A. El'yashevich, *Atomic and Molecular Spectroscopy* (Nauka, Moscow, 1962), 889 pp; *Physical Encyclopedic Dictionary* (Moscow, 1995).
2. V.E. Zuev, *Transparency of the Atmosphere for Visible and IR-Radiation* (Sov. Radio, Moscow, 1966), 496 pp.
3. Yu.S. Makushkin, "Intramolecular interactions and infrared spectra of atmospheric gases," Author's Abstract of Doct. Phys.-Math. Sci. Dissert., Tomsk (1977), 40 pp;

- M.R. Aliev, "Investigations into the theory of vibrational-rotational spectra of polyatomic molecules," Author's Abstract of Doct. Phys.-Math. Sci. Dissert., Moscow (1977), 45 pp.
4. W. Baumann and R. Mecke, *Zs. f. Phys.* **81**, 445–464 (1933); K. Frandenberg and R. Mecke, *Zs. f. Phys.* **81**, 465–481 (1933).
5. G. Herzberg, J.M.T. Spinks, *Zs. f. Phys.* **91**, 388–399 (1934); G.W. Funke and G. Herzberg, *Phys. Rev.* **49**, 100–112 (1936); G. Herzberg, L. Herzberg, *J. Opt. Soc. Am.* **43**, No. 11, 1037–1044 (1953).
6. V.I. Kravchenko, M.S. Soskin, and V.V. Tarabrov, *Pis'ma Zh. Eksp. Teor. Fiz.* **5**, No. 10, 355–356 (1967).
7. R.N. Dike, *Phys. Rev.*, No. 2, 472–473 (1953).
8. M.L. Strekalov and A.I. Burshtein, *Zh. Eksp. Teor. Fiz.* **61**, No. 1(7), 101–111 (1971); A.I. Burshtein, M.L. Strekalov, and S.I. Temkin, *Zh. Eksp. Teor. Fiz.* **66**, No. 3, 894–906 (1974); A.I. Burshtein and G.L. Smirnov, *Zh. Eksp. Teor. Fiz.* **65**, No. 6, 2174–2184 (1973).
9. E.G. Pestov and S.G. Rautian, *Zh. Eksp. Teor. Fiz.* **64**, No. 6, 2032–2045 (1973).
10. S.G. Rautian, G.I. Smirnov, and A.M. Shalagin, *Nonlinear Resonances in the Spectra of Atmos. and Molecules* (Nauka, Novosibirsk, 1979), 310 pp.
11. A.P. Kol'chenko and S.G. Rautian, *Zh. Eksp. Teor. Fiz.* **54**, No. 4, 959–973 (1968); A.I. Burshtein, *ibid.*, 1120–1131.
12. U. Fano and L. Fano, *Atomic and Molecular Physics* [Russian translation] (Nauka, Moscow, 1980), 651 pp.; V.S. Letokhov and V.P. Chebotaev, *Principles of Nonlinear Laser Spectroscopy* (Nauka, Moscow, 1975), 279 pp.; L.V. Vilkov and Yu.A. Pentin, *Physical Methods of Investigations as Applied to Chemistry* (Shkola, Moscow, 1987), 359 pp.
13. B.A. Zon and B.G. Kantsel'son, *Zh. Eksp. Teor. Fiz.* **69**, No. 4(10), 1166–1178 (1975); V.P. Makarov and M.V. Fedorov, *Zh. Eksp. Teor. Fiz.* **70**, No. 4, 1185–1196 (1976); R.Z. Vitlina and A.V. Chaplik, *ibid.*, No. 6, 2127–2132.
14. F.Kh. Gel'mukhanov, *Pis'ma Zh. Eksp. Teor. Fiz.* **46**, No. 2, 57–59 (1987).
15. A.M. Shalagin, *Pis'ma Zh. Eksp. Teor. Fiz.* **30**, No. 6, 330–333 (1979).
16. P.A. Apanasevich, *Fundamentals of the Theory of Light Interaction with Matter* (Nauka i Tekhnika, Minsk, 1997), 496 pp.
17. S.A. Akhmanov, in: *Nonlinear spectroscopy*, N.M. Blombergen, ed. (Mir, Moscow, 1979), 586 pp.
18. A.N. Oraevskii, A.A. Stepanov, and O.A. Shcheglov, *Zh. Eksp. Teor. Fiz.* **69**, No. 6(12), 1991–2025 (1975); E.B. Aleksandrov, *Opt. Spektr.* **14**, No. 3, 436–438 (1963); *ibid.* **19**, No. 3, 452–455 (1965); *Uspekhi Fiz. Nauk* **107**, No. 4, 595–622 (1972).
19. N.V. Perel'man, V.A. Kovarskii, and I.Sh. Averbukh, *Zh. Eksp. Teor. Fiz.* **80**, No. 1, 80–95 (1981).
20. V.M. Akulin and N.V. Karlov, *Strong Resonance Interactions in Quantum Electronics* (Nauka, Moscow, 1987), 311 pp.
21. V.E. Shapiro, *Zh. Eksp. Teor. Fiz.* **89**, No. 6(12), 1957–1973 (1985).
22. D.G. Akopyan, "Theory of resonance self-action and four-wave interactions considering the magnetic sublevels relaxation," Author's Abstract of Cand. Phys.-Math. Sci. Dissert., Erevan (1986), 16 pp.; A.P. Kazantsev, V.S. Smirnov, A.M. Tumaikin, and I.A. Yagofeev, *Quantum Theory of the Atomic Multipole Moment Relaxation and its Applications to Problems of Light Absorption from the Ground State*, Preprint No. 5, Institute of Atmospheric Optics of the SB AS of the USSR, Tomsk (1982), 44 pp.
23. G.A. Askar'yan and V.A. Namiot, *Zh. Eksp. Teor. Fiz.* **89**, No. 69, 1986–1990 (1975).
24. C.E. Moore, M.G. Minnaert, and J. Houtgest, *Solar Spectrum 2935 to 8770 Å*, National Bureau of Standards, USA (1966).
25. L. Delbouille, G. Roland, and L. Neven, *Photometric Atlas of the Solar Spectrum from 3000 to 10000 Å*, Institut d'Astrophysique de L'Universite de Liege (1973).
26. J.W. Swensson, W.S. Benedict, L. Delbouille, and G. Roland, *The Solar Spectrum from 7498 to 12016 Å. Table of Measures and Identification*, Liege (1970).
27. L.A. Pakhomycheva, E.A. Sviridenkov, and A.S. Suchkov, *Pis'ma Zh. Eksp. Teor. Fiz.* **12**, No. 2, 60–63 (1970); V.M. Baev, V.Ya. Gulov, E.A. Sviridenkov, and M.P. Frolov, *Kvant. Elektron.* **2**, No. 6, 1328–1331 (1975); E.N. Antonov, V.A. Kalashnikov, and V.P. Mironenko, *Usp. Fiz. Nauk* **117**, No. 3, 547–576 (1975).
28. L.S. Rothman, R.R. Gamache, A. Golman, et al., *J. Quant. Spectrosc. Radiat. Transfer* **48**, 469–507 (1992).
29. M.M. Makogon and A.M. Solodov, *Pis'ma Zh. Tekhn. Fiz.* **4**, No. 4, 309–312 (1978); *ibid.* **3**, No. 15, 767–770 (1977).
30. A.B. Antipov, A.D. Bykov, O.K. Voitsekhovskaya, et al., *Dokl. Akad. Nauk SSSR* **251**, No. 1, 67–70 (1980); A.B. Antipov, A.D. Bykov, V.E. Zuev, et al., *J. Mol. Spectrosc.* **89**, Nos. 1–3, 449–459 (1981).
31. V.P. Lopasov, "Laser spectroscopy of molecules in the visible and near-IR ranges and its application to atmospheric optics," Author's Abstract of Doct. Phys.-Math. Sci. Dissert., Tomsk (1982), 26 pp.
32. A.D. Bykov, V.P. Lopasov, Yu.S. Makushkin, et al., *J. Mol. Spectrosc.* **94**, No. 1, 1–27 (1982); L.N. Sinitisa, "High-sensitive laser spectroscopy of high-lying vibrational-rotational molecule states," Author's Abstract of Doct. Phys.-Math. Sci. Dissert., Tomsk (1988), 33 pp.
33. A.D. Bykov, V.E. Zuev, V.P. Lopasov, et al., *Dokl. Akad. Nauk SSSR* **258**, No. 4, 854–858 (1981); A.D. Bykov, V.A. Kapitanov, O.V. Naumenko, et al., *J. Mol. Spectrosc.* **153**, No. 1, 197–207 (1992); A.D. Bukov, O.V. Naumenko, M.A. Smirnov, et al., *Can. J. Phys.* **72**, No. 1, 989–1000 (1994).
34. A.D. Bykov, "Analysis of water vapor absorption spectrum in short-wavelength region," Author's Abstract of Doct. Phys.-Math. Sci. Dissert., Institute of Atmospheric Optics of the Siberian Branch of the Academy of Sciences of the USSR, Tomsk (1994).
35. A.D. Bykov, O.V. Naumenko, and L.N. Sinitisa, *Atm. Opt.* **3**, No. 10, 1014–1019 (1990).
36. C. Camy-Peyret, J.-M. Flaund, J.-Y. Mandin, et al., *J. Mol. Spectrosc.* **113**, No. 2, 208–228 (1985).

37. A.D. Bykov, V.S. Makarov, N.I. Moskalenko, et al., *J. Mol. Spectrosc.* **123**, No. 1, 126 (1987).
38. V.P. Lopasov and L.N. Sinitsa, *Zh. Prikl. Spektrosk.* **28**, No. 1, 60–63 (1978); V.E. Zuev, V.P. Lopasov, and L.N. Sinitsa, *Opt. Spektrosk.* **45**, No. 3, 590–593 (1978); V.E. Zuev, V.P. Lopasov, L.N. Sinitsa, and A.M. Solodov, *Dokl. Akad. Nauk SSSR* **256**, No. 5, 1109–1111 (1981); V.E. Zuev, V.P. Lopasov, L.N. Sinitsa, and A.M. Solodov, *J. Mol. Spectrosc.* **94**, Nos. 1–3, 208–209 (1982).
39. V.P. Lopasov, L.N. Sinitsa, and A.M. Solodov, *Opt. Spektrosk.* **49**, No. 4, 828–830 (1980).
40. L.N. Sinitsa, *Atmos. Oceanic Optics* **8**, Nos. 1–2, 80–92 (1995).
41. A.D. Bykov, Yu.S. Makushkin, V.I. Serdyukov, et al., *J. Mol. Spectrosc.* **104**, No. 3, 297–307 (1984); P.S. Ormsby, K.N. Rao, M. Winniwasser, et al., *J. Mol. Spectrosc.* **158**, No. 1, 109 (1993).
42. A.D. Bykov, O.V. Naumenko, L.N. Sinitsa, et al., *J. Mol. Spectrosc.* **172**, No. 2, 243–253 (1995).
43. V.I. Perevalov, "Method of effective operators as applied to the theory of molecular spectra," Author's Abstract Doct. Phys.-Math. Sci. Dissert., Institute of Atmospheric Optics of the Siberian Branch of the Russian Academy of Sciences, Tomsk (1996); J.L. Teffo, V.I. Perevalov, and O.M. Lyulin, *J. Mol. Spectrosc.* **168**, No. 2, 390–403 (1994); A. Comparque, D. Pemogorov, M. Bach, et al., *J. Chem. Phys.* **103**, 5931–5938 (1995).
44. V.E. Zuev, V.P. Lopasov, and I.S. Tyryshkin, *Kvant. Elektron.* **4**, No. 6, 1375–1377 (1977).
45. V.P. Lopasov and I.S. Tyryshkin, *Zh. Prikl. Spektrosk.* **28**, No. 1, 360–363 (1976); A.P. Godlevskii, M.M. Makogon, and I.S. Tyryshkin, *Zh. Prikl. Spektrosk.* **24**, No. 1, 132–135 (1976).
46. V.P. Lopasov, S.F. Luk'yanenko, Yu.N. Ponomarev, and B.A. Tikhomirov, *Zh. Prikl. Spektrosk.* **33**, No. 2, 365–367 (1980).
47. B.E. Grossman, E.V. Browell, A.D. Bykov, et al., *Atm. Opt.* **3**, No. 7, 617–630 (1990);
48. A.D. Bykov, Yu.N. Ponomarev, and L.N. Sinitsa, *Atmos. Oceanic Opt.* **5**, No. 9, 604–608 (1992).
49. Yu.N. Ponomarev and B.A. Tikhomirov, *Opt. Spektrosk.* **58**, No. 4, 947–948 (1985).
50. A.D. Bykov, E.A. Korotchenko, Yu.S. Makushkin, et al., *Opt. Atm.* **1**, No. 1, 40–45 (1988).
51. B.G. Ageev, Yu.N. Ponomarev, B.A. Tikhomirov, *Nonlinear Opto-Acoustic Spectroscopy of Molecular Gases* (Nauka, Novosibirsk, 1987), 128 pp.
52. Yu.N. Ponomarev and S.B. Ponomareva, *Opt. Spektrosk.* **51**, No. 3, 529–534 (1981).
53. V.E. Zuev, V.P. Lopasov, and Yu.N. Ponomarev, *Dokl. Akad. Nauk SSSR* **231**, No. 5, 1106–1108 (1976); *ibid.* **239**, No. 6, 1320–1322 (1978).
54. V.P. Lopasov, Yu.N. Ponomarev, and B.A. Tikhomirov, *Kvant. Elektron.* **9**, No. 8, 1724–1727 (1982).
55. V.E. Zuev, Yu.N. Ponomarev, and B.A. Tikhomirov, *Dokl. Akad. Nauk SSSR* **277**, No. 2, 347–350 (1984).
55. E.A. Ryabov, *Kvant. Elektron.* **2**, No. 1, 138–140 (1975).
56. V.E. Zuev, V.P. Lopasov, and M.M. Makogon, *Dokl. Akad. Nauk SSSR* **199**, No. 5, 1041–1043 (1971); V.E. Zuev, V.P. Lopasov, and M.M. Makogon, *Appl. Opt.* **10**, No. 10, 1015–1020 (1971).
57. R.K. Long, Ohio State Univ. Engineering Publication Bull, No. 199, 24 (1996).
58. T.A. Wiggins, E.K. Plyer, and E.D. Tidwell, *J. Opt. Soc. Am.* **53**, No. 3, 589–595 (1963).
59. V.P. Kochanov, V.P. Lopasov, and S.F. Luk'yanenko, *Izv. Akad. Nauk SSSR. Ser. Fiz.* **49**, No. 3, 516–520 (1985).
60. V.M. Klimkin and V.N. Fedorishchev, *Opt. Atm.* **1**, No. 7, 72–76 (1988); *ibid.* **1**, No. 8, 26–30; *Atm. Opt.* **2**, No. 2, 174–175 (1989).
61. V.M. Klimkin, S.F. Luk'yanenko, I.N. Potapkin, and V.N. Fedorishchev, *Atm. Opt.* **2**, No. 3, 258–259 (1989); S.F. Luk'yanenko, T.I. Novakovskaya, and I.N. Potapkin, *ibid.* **2**, No. 7, 579–582 (1989).
62. S.E. Karmazin, A.N. Kuryak, M.M. Makogon, and A.L. Tsvetkov, *Atmos. Oceanic Optics* **8**, No. 11, 937–939 (1995).
63. I.M. Al'tshul', V.P. Lopasov, and S.D. Tvorogov, "Propagation of Waves Satisfying the Conditions of the Rabi Resonance through a Two-Level Medium," Preprint No. 67, Institute of Atmospheric Optics of the Siberian Branch of the Academy of Sciences of the USSR, Tomsk (1988), 23 pp.; S.D. Tvorogov, V.G. Fedoseev, and K.N. Yugai, *Atm. Opt.* **4**, No. 6, 453–457 (1991).
64. V.P. Kochanov and M.S. Zubova, *Zh. Eksp. Teor. Fiz.* **101**, No. 6, 1772–1786 (1992); *ibid.* **105**, No. 3, 499–514 (1994).
65. V.P. Lopasov, *Atmos. Oceanic Optics* **9**, No. 8, 734–736 (1996).
66. S.D. Tvorogov, *Izv. Vyssh. Uchebn. Zaved. Ser. Fiz.*, No. 10, 93–103 (1996).